

A Separable Approximation to DSI Deconvolution

Michael Paquette¹ and Maxime Descoteaux¹

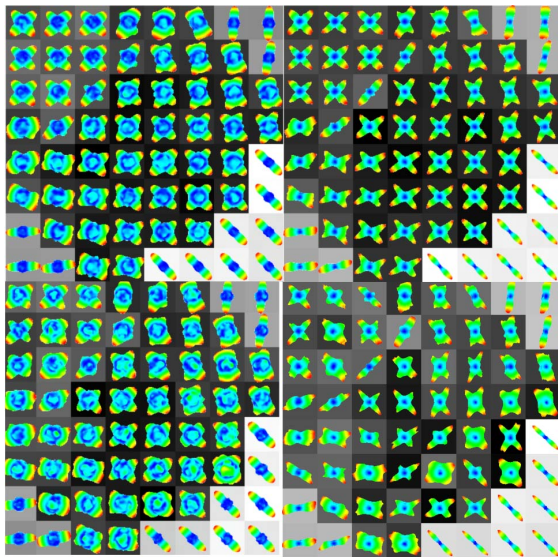
¹SCIL, Université de Sherbrooke, Sherbrooke, Quebec, Canada

Introduction : Diffusion Spectrum Imaging (DSI) is becoming central in many connectomics study [1] and it is important to better understand the hidden underlying image processing steps involved in the reconstruction before one can robustly use it for tractography and connectomics studies. DSI is a model free Diffusion Magnetic Resonance Imaging (dMRI) technique that allows reconstruction of a diffusion Ensemble Average Propagator (EAP) from a Cartesian grid q-space sampling. This approach is based on the Fourier relationship between the EAP and the diffusion signal across the whole continuous q-space. However, in practice, the use of a maximum b-value and a finite number of samples leads to a modified EAP convolved with a known Point Spread Function (PSF). We can compute that PSF by taking the Fourier Transform (FT) of the q-space sampling scheme [2]. In classical DSI acquisitions [3], we sample the 515 points of a cubic lattice lying within a sphere of five lattice units in radius. The resulting PSF is the discrete FT (dFT) of the binary mask of that sphere leading to a non-separable 3D sinc convolution filter. In this work, we propose a new separable filter approximating the true PSF allowing us to use a regularized deconvolution of the propagator with least-square 1D approach.

Methods : The diffusion propagator $\mathbf{P}(\mathbf{r})$ and the normalized diffusion signal $\mathbf{E}(\mathbf{q})=\mathbf{S}(\mathbf{q})/S(0)$ share a Fourier relationship but the actual measured EAP during a DSI acquisition is given by $\mathbf{P}_m(\mathbf{r})$, where $*$ is the convolution operator (see box). If a 3D filter \mathbf{G}_s can be expressed by the outer tensor multiplication of three 1D filters such that $G_s(i,j,k)=g_x(i)g_y(j)g_z(k)$ then \mathbf{G}_s is a separable filter. Can we approximate the DSI non-separable PSF filter by separable one? We first look into the 2D problem. It is well known that any matrix that can be expressed as the outer product of two vectors is of rank one. Hence, we can approximate the 2D filter \mathbf{G} by the closest rank one matrix $\mathbf{G}\mathbf{1}$ (see box). By the Eckart-Young theorem [4], the truncated singular value decomposition (SVD) of \mathbf{G} with all but the largest singular value set to zero is the analytical solution : $\mathbf{G}\mathbf{1}=\mathbf{U}(\mathbf{E}\mathbf{1})\mathbf{V}^T$ where $\mathbf{G}=\mathbf{U}\mathbf{E}\mathbf{V}^T$ is the SVD decomposition of \mathbf{G} and \mathbf{E}_n is \mathbf{E} truncated to the n largest singular value. Since the notion of rank and SVD decomposition is not generalized for 3D matrices, we take the central 2D slice of the numerical 3D filter to compute our 1D filter with the above method. In practice, our numerical 3D filter \mathbf{G} is obtained by taking the dFT of our q-space sampling binary mask \mathbf{B} , $\mathbf{G}=\mathbf{FFT}(\mathbf{B})$, leading to \mathbf{G} being symmetric along all Cartesian axes as long as the acquisition scheme is symmetric, which is the case of classical DSI. Looking at the separable convolution formula $\mathbf{S}*\mathbf{G}\mathbf{1}=(\mathbf{S}*g)*g^T=(\mathbf{S}*g^T)*g$, it is clear that separable deconvolution is applicable. We first implement the convolution as a matrix multiplication by building the matrix \mathbf{M} where the i th row are the values of the filter \mathbf{g} centered on the i th column, $\mathbf{M}\mathbf{S}=\mathbf{S}*g$. The 1D deconvolution problem can now be expressed in terms of regularized Tikhonov least-square (see box) with solution $\mathbf{S}_a=(\mathbf{M}^T\mathbf{M} + c\mathbf{I})^{-1}\mathbf{M}^T\mathbf{S}$ from the Moore-Penrose pseudo-inverse with $(c\mathbf{I})$ the identity matrix times a constant. Now, to perform 3D deconvolution, we simply used our approximated 1D filter to build the matrix \mathbf{M} and then the solution matrix with the pseudo-inverse. Then, for a given Cartesian axis, we deconvolve each row by multiplying it with the system matrix, we then repeat for the second Cartesian axis and finally for the third. The non-smoothness of the discretized filter can lead to negative propagator values and artifacts aligned with the Cartesian axes due to the nature of the rank approximation. To correct these deconvolution artifacts that lead to physically meaningless EAPs, a thresholding strategy imposing radial monotonic decays is applied on the deconvolved propagators.

$$\begin{aligned}
 P(\vec{r}) &= \iiint E(\vec{q}) e^{-2\pi i \vec{r} \cdot \vec{q}} d\vec{q} \\
 P_m(\vec{r}) &= \iiint |E(\vec{q})| e^{-2\pi i \vec{r} \cdot \vec{q}} d\vec{q} \\
 &= \iiint_{\|\vec{q}\| \leq q_{max}} (|E(\vec{q})| \cdot M_{q_{max}}(\vec{q})) e^{-2\pi i \vec{r} \cdot \vec{q}} d\vec{q} \\
 &= (P * \mathcal{F}(M_{q_{max}}(\vec{q})))[\vec{r}] \\
 M_{q_{max}}(\vec{q}) &= \begin{cases} 1 & : \|\vec{q}\| \leq q_{max} \\ 0 & : \|\vec{q}\| > q_{max} \end{cases} \\
 G\mathbf{1} &= \arg \min_H \|G - H\|_F \\
 &\quad \text{s.t. rank}(H) = 1 \\
 s_d &= \arg \min_{s_a} \frac{1}{2} \|M s_a - S\|_2^2 + \frac{c}{2} \|s_a\|_2^2
 \end{aligned}$$

Dataset : The data used for this abstract comes from the a multi-tensor model field used in the *ISBI 2012 HARDI reconstruction Challenge* [6]. It is composed of three simulated bundle with tensor of FA = 0.8 with diffusivities = {[17.25 3.03 3.03];[12.52 2.20 2.20];[10.40 1.83 1.83]} x 1e-4 mm²/s. The field used is the crossing of the first straight bundle with the arced third bundle leading to various angles of crossings. The raw diffusion signal is generated using a classical full Cartesian grid with 515 measurements [3] and bmax=6000 s/mm².



Results : As seen in the figure, the ODFs computed with the method are much sharper and accurate than those obtained from DSI. Even at low SNR, the underlying structure of the field is visible. The generalized fractional anisotropy (GFA) is significantly higher and closer to the ground truth after the deconvolution. We computed the normalized mean squared error (NMSE) of the GFA maps and for SNR=[inf, 30, 20, 10], we obtained NMSE = [0.077, 0.081, 0.084, 0.107] with DSI and NSME = [0.011, 0.012, 0.013, 0.036] with the deconvolution, a 3-fold increase in accuracy for any SNR.

Discussion : The deconvolution of DSI propagators has already been studied in Canales et al. [2], where they used the Lucy-Richardson algorithm to perform a 3D deconvolution. In their work, they approximate the true 3D sinc filter with a gaussian and get an increase in angular resolution of the computed ODF but their propagators are no longer physically meaningful and radially monotone. Nonetheless, ODFs are sharp and are tailored to give fiber ODF-like angular profiles, which seem the best candidate for fiber tracking. In this work, by approximating the true sinc filter, we aim to correct the artefacts (ringing, blur) in the propagator related to the truncation of q-space. Our EAPs are accurate and our computed ODFs closest to the ground truth DSI diffusion ODFs. Hence, if one is interested in EAP metrics [5], our deconvolved EAP seems the best candidate. We believe that DSI reconstruction should not be used as a black box as there remains several open processing questions towards optimal DSI reconstruction. Future work will look into advanced optimisation scheme to constrain the deconvolution.

On the left the DSI-ODFs and on the right the ODFs from our method, onwork will look into advanced optimisation scheme to constrain the deconvolution. the top SNR=20, on the bottom SNR=10. Backgrounds are GFA maps.

References : [1] Hagmann et al. J. Neuro. Meth. 2010. [2] Canales et al. Neuroimage 2010. [3] Wedeen et al. MRM 2005. [4] Eckart and Young. Psychometrika 1936. [5] Hosseinbor et al. MICCAI 2012. [6] http://hardi.epfl.ch/static/events/2012_ISBI/